High-excitation effect on photoluminescence of sol-gel ZnO nanopowder

C. H. Chia, Y. J. Lai, T. C. Han, J. W. Chiou, Y. M. Hu, and W. C. Chou

Articles you may be interested in

Structural, optical, vibrational, and magnetic properties of sol-gel derived Ni doped ZnO nanoparticles
J. Appl. Phys. **114**, 033912 (2013); 10.1063/1.4813868

Surface related and intrinsic exciton recombination dynamics in ZnO nanoparticles synthesized by a sol-gel method
Appl. Phys. Lett. **102**, 013109 (2013); 10.1063/1.4774002

Biexciton emission from sol-gel ZnMgO nanopowders
Appl. Phys. Lett. **96**, 191902 (2010); 10.1063/1.3428780

Structural and photoluminescence properties of ZnO thin films prepared by sol-gel process
J. Appl. Phys. **104**, 113539 (2008); 10.1063/1.3021358

Effects of Mg incorporation on the optical properties of ZnO prepared by the sol-gel method
J. Appl. Phys. **103**, 113709 (2008); 10.1063/1.2939255

High-excitation effect on photoluminescence of sol-gel ZnO nanopowder

C. H. Chia,[1,a)] Y. J. Lai,[1] T. C. Han,[1] J. W. Chiou,[1] Y. M. Hu,[1] and W. C. Chou[2]
[1]*Department of Applied Physics, National University of Kaohsiung, Kaohsiung 81148, Taiwan*
[2]*Department of Electrophysics, National Chiao Tung University, Hsin-Chu 30010, Taiwan*

We studied the power-dependent photoluminescence of ZnO nanopowder grown by sol-gel method at low temperature. At moderate optical pumping intensity, two nonlinear emission bands due to the radiative recombination of free biexciton and the inelastic exciton–exciton scattering were detected. We found that the threshold of the excitation density for the emergence of the nonlinear emission bands is low (<18 W/cm^2) in sol-gel ZnO nanopowders. © *2010 American Institute of Physics*. [doi:10.1063/1.3327338]

It is well established that the interaction between two excitons will lead to the formation of biexcitons and the inelastic scattering between excitons. These exciton–exciton interactions will cause the emergence of nonlinear emission lines at the low-energy side of excitonic emission.[1–5] ZnO has been attracting much attention due to its potential applications in ultraviolet optoelectronics devices. The large exciton binding energy of ZnO (60 meV) (Ref. 6) enables the utilization of exciton-related transitions in light-emitting devices even at room-temperature (RT). In ZnO quantum well, the binding energy of biexcitons and the exciton–exciton scattering efficiency enhance significantly.[7,8] In particular, the biexciton binding energy in ZnO quantum well can be comparable to thermal energy of RT,[8] indicating the possibility of biexciton lasing at even at RT.[9,10] Therefore, study of photoluminescence (PL) of the highly excited ZnO is important.

Sol-gel technique is much cheaper and easier to grow large area of ZnO films than much sophisticated techniques. The sol-gel ZnO thin films have already been realized in transparent p-n junction diodes[11] and transistors.[12] For a large use of sol-gel ZnO for optoelectronic devices, a better understanding of the PL mechanisms in sol-gel ZnO under high-excitation condition is necessary. In this letter, we report the PL of highly excited sol-gel ZnO nanopowders. At moderate optical pumping intensity, two nonlinear emission bands due to the radiative recombination of free biexciton and the inelastic exciton–exciton scattering were found.

The ZnO nanopowders were grown from aqueous solution prepared using zinc nitrate hexahydrate [$Zn(NO_3)_2 \cdot 6H_2O$] as the starting material, de-ionized water as the solvent, and citric acid ($C_6H_8O_7$) as the stabilizer. The precursor solution was mixed thoroughly with a magnetic stirrer in 80 °C water bath until the formation of a sol. The sol was preheated in a furnace at 120 °C for 12 h to evaporate the solvent and remove the organic residuals. The powders obtained from the dried sol were then annealed at 600 °C for 2 h at ambient air. The crystalline size of the ZnO nanopowders was estimated to be about 30 nm by Sherrer's equation from the result of x-ray diffraction method using a monochromatized x-ray beam $CuK_\alpha = 0.154$ nm. No quantum confinement effect of excitons is expected in the sample.

The PL spectra were measured by a 32-cm-long monochromator and a charge-coupled device camera. The pump source for the low-excitation spectra was mercury lamp. The excitation-power dependence of the PL spectra was measured by the 266 nm-line of an neodymium-doped yttrium aluminium garnet (Nd:YAG) laser. The pulsed laser has a pulse width of 10 ns and a repetition rate of 20 Hz. The reflection spectrum was obtained by using a deuterium-tungsten lamp. A closed cycle refrigerator was used to perform the T-dependent measurement.

Figure 1 shows the low-T spectra of ZnO nanopowders. The reflection spectrum and low-excitation PL spectrum (80 μW/cm^2) were shown in Fig. 1(a). The reflection spectrum shows three distinct anomalies in the exciton resonance region, the minimum energies of which are 3.378, 3.384, and 3.436 eV. These can be assigned to the ground states of A, B,
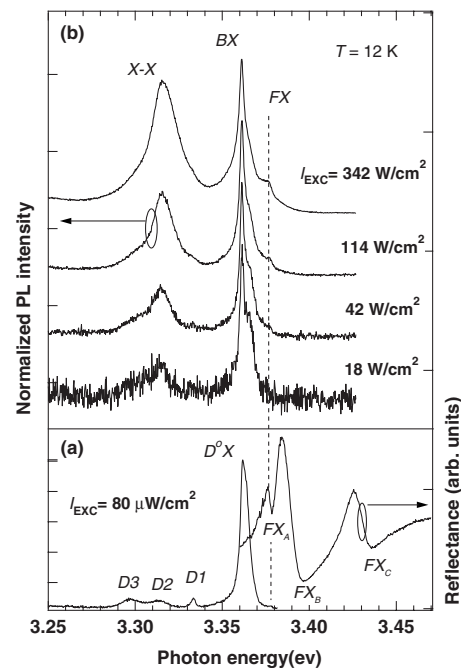

FIG. 1. (a) Low-excitation PL spectrum and reflection spectrum of ZnO nanopowders taken at $T=12$ K. FX_A, FX_B, and FX_C represented the energies of free A, B, and C excitons, respectively. The origins of the emission band D^0X, $D1$, $D2$, and $D3$ are given in text. (b) Evolution of PL spectra in ZnO nanopowders with increasing excitation intensity taken at 12 K. BX and $X-X$ emission lines are due to the radiative recombination of biexcitons and inelastic exciton–exciton scattering.

a)Author to whom all correspondence should be addressed. Electronic mail: chchia@nuk.edu.tw.
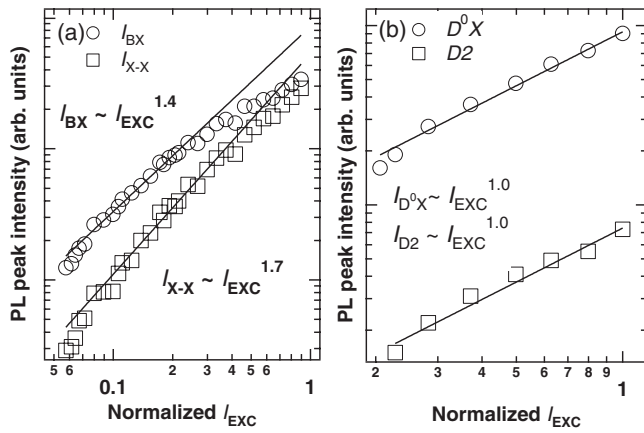
FIG. 2. (a) Evolution of peak intensities of BX emissions (open circles) and $X-X$ emission (open squares) from ZnO nanopowders, excited by Nd:YAG laser. Here, the maximum $I_{EXC} = 342$ W/cm^2. The solid lines represent the power law dependence $I_{BX} \sim I_{EXC}^{1.4}$ and $I_{X-X} \sim I_{EXC}^{1.7}$. (a) Evolution of peak intensities of D^0X emissions (open circles) and $D2$ emission (open squares) from ZnO nanopowders, excited by mercury lamp. Here, maximum $I_{EXC} = 80$ μW/cm^2. The solid lines represent the power law dependence $I_{DX} \sim I_{EXC}^{1.0}$ and $I_{D2} \sim I_{EXC}^{1.0}$.

FIG. 3. T-dependent PL spectra of ZnO nanopowders under $I_{EXC} = 139$ W/cm^2. The open circles label the biexciton emission. The emission completely disappears at $T = 180$ K.

and C free exciton (FX), respectively.[6,13–15] It is well known that the allowed selection rule for the optical transitions of A and B excitons is $E \perp c$, the existence of C-exciton structure in the reflectance spectrum indicates the c-axis orientation is different from grain to grain in our sample.

The radiative recombination of donor-bound exciton D^0X (3.362 eV) dominates the low-excitation PL spectrum. Three emission bands were found at the low-energy side of the main PL band. The energetic positions of $D1$, $D2$, and $D3$ emission peak are 3.334, 3.313, and 3.297 eV, respectively. The $D1$ and $D2$ emissions can be attributed to the transitions related to the structural defects, whereas the $D3$ band may due to the two-electron satellite of the D^0X.[16]

In Fig. 1(b), the evolution of PL band as a function of excitation power (I_{EXC}) was shown. As the I_{EXC} increases, two emission bands with peak energies of 3.361 eV (denotes as BX) and 3.315 eV (denotes as $X-X$), dominate the PL spectra. Although the energetic positions of these two bands are almost the same as that of the D^0X and $D2$, we believe that the emissions mainly originated from the radiative recombination of biexcitons (BX) and inelastic exciton–exciton ($X-X$) scattering for the high I_{EXC} condition, as will be verified later. A shoulder appears at the high-energy side of the BX band as the I_{EXC} increases. This shoulder could be attributed to the transition of FXs because the bound exciton states saturate under the high I_{EXC} condition.

Figure 2(a) shows the PL peak intensities of the BX (I_{BX}) and $X-X$ (I_{X-X}) bands as a function of I_{EXC} (with maximum value of 342 W/cm^2). We found that the I_{BX} and I_{X-X} increase superlinearly with the I_{EXC}, with $I_{BX} \propto I_{EXC}^{1.4}$ and $I_{X-X} \propto I_{EXC}^{1.7}$. The biexcitonic transition energy is given by $E_{BX} = 2E_{FX} - E_{BX}^b$, with E_{FX} and E_{BX}^b being the free exciton energy and the free biexciton binding energy. We can obtain the lowest resonance energy of A-exciton states by subtracting the longitudinal-transverse splitting energy (2 meV) (Ref. 6) from the reflectance minimum energy of A-exciton (3.378 eV) in Fig. 1(a). The E_{BX}^b of ZnO is about 15 meV.[1,17] Therefore, the resonance energy of biexciton transitions should be 3.361 eV. Also, at high I_{EXC}, the inelastic collision between
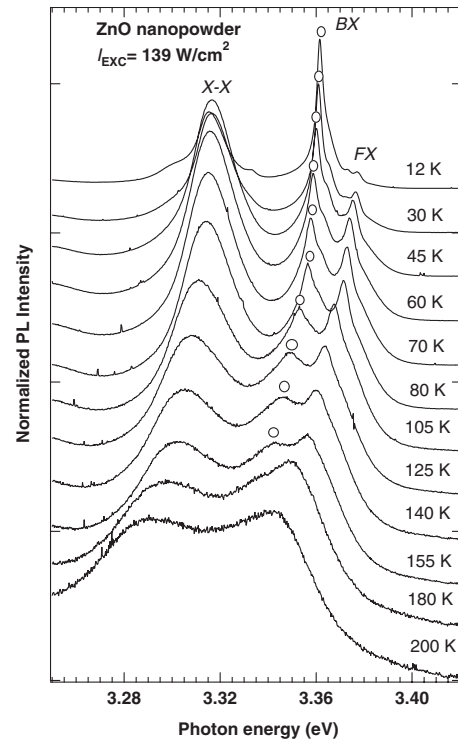
two excitons could result an exciton excited into a continuum states, and a photon with energy given by $E_{X-X} = E_{FX} - E_{FX}^b - 1.5k_BT$,[18] with E_{FX}^b (60 meV) and k_B being the free exciton binding energy and the Boltzmann constant. At 10 K, the thermal energy is about 1 meV. Therefore, the E_{X-X} is 3.315 eV. The measured peak energies of the BX and $X-X$ bands coincide well with the calculations. Since the I_{BX} and I_{X-X} depends superlinearly on the I_{EXC}, we believe that the dominant PL bands are due to the radiative recombination of biexcitons and inelastic exciton–exciton scattering under the high I_{EXC} condition.

Figure 2(b) shows the evolution of the peak intensities of $D2$ and D^0X, as a function of I_{EXC} (with maximum value of 80 μW/cm^2). We used the mercury lamp as an excitation source and a variable neutral density filter to monitor the pumping intensity. Both of them show a linear dependence on I_{EXC}. Therefore, at extremely low-excitation, it is reasonable to assign the $D2$ and D^0X bands to structural defects and donor-bound excitons, respectively. However, the BX and $X-X$ bands overlapped the $D2$ and D^0X bands at the high excitation density. This also explains why the I_{BX} and I_{X-X} do not follow the quadratic dependence on I_{EXC}.

Figure 3 shows the T-dependent PL of ZnO nanopowders ($I_{EXC} = 139$ W/cm^2). As T increases, all of the emission band redshift. We can observe the intensity of the biexciton transition gradually decreases, and finally diminishes at $T = 180$ K, of which the thermal energy is corresponding to the $E_{BX}^b \sim 15$ meV.

The PL of ZnO associated with various exciton transitions has been investigated by several research groups.[1–3,7–9] We note that the threshold-I_{EXC} for the emergence of the nonlinear BX and $X-X$ emission bands is at least lower than 18 W/cm^2. The threshold-I_{EXC} for the emergence of BX band might be comparable to that reported in Ref. 15, but

significantly lower than that reported in Ref. 5. Furthermore, it is surprising that the threshold-I_{EXC} for the $X-X$ emission band is also very low, compared to that reported in Ref. 19 and 20. Indeed, Pan *et al.*[2] has reported the *BX* and $X-X$ emission bands from sol-gel ZnO powder, excited by an cw-He-Cd laser. This implies the high efficiency of biexciton formations and inelastic exciton–exciton scattering in the sol-gel sample. We tentatively interpret the low threshold-I_{EXC} as being due to the nanocrystalline nature of the sample. When the crystal size is smaller than the Bohr radius of exciton (1.8 nm in ZnO) but larger than the excitonic coherence length, an exciton wave function can coherently extend over the nanocrystalline powders. This can lead to a large enhancement in the exciton oscillator strength.[21]

In summary, we studied the PL of highly excited sol-gel ZnO nanopowders at low-*T*. The nonlinear emissions due to free biexciton transitions and inelastic exciton–exciton scattering were observed as the I_{EXC} increases. We found that the threshold of the I_{EXC} for the emergence of the nonlinear emission bands is low (<18 W/cm^2), indicating a high efficiency of exciton–exciton interactions in the sol-gel ZnO nanopowders.

[1] H. J. Ko, Y. F. Chen, T. Yao, K. Miyajima, A. Yamamoto, and T. Goto, Appl. Phys. Lett. **77**, 537 (2000).
[2] C. J. Pan, K. F. Lin, and W. F. Hsieh, Appl. Phys. Lett. **91**, 111907 (2007).
[3] H. D. Sun, T. Makino, Y. Segawa, M. Kawasaki, A. Ohtomo, K. Tamura, and H. Koinuma, Appl. Phys. Lett. **78**, 3385 (2001).
[4] R. A. R. Leute, M. Feneberg, R. Sauer, K. Thonke, S. B. Thapa, F. Scholz, Y. Taniyasu, and M. Kasu, Appl. Phys. Lett. **95**, 031903 (2009).
[5] F. Y. Jen, Y. C. Lu, C. Y. Chen, H. C. Wang, C. C. Yang, B. P. Zhang, and Y. Segawa, Appl. Phys. Lett. **87**, 072103 (2005).
[6] E. Mollwo, in *Semiconductors: Physics of II-VI and I-III Compounds, Semimagnetic Semiconductors*, Landolt-Börnstein New Series Vol. 17, edited by O. Madelung, M. Schulz, and H. Weiss (Springer, Berlin, 1982), p. 35.
[7] H. D. Sun, T. Makino, N. T. Tuan, Y. Segawa, Z. K. Tang, G. K. L. Wong, M. Kawasaki, A. Ohtomo, K. Tamura, and H. Koinuma, Appl. Phys. Lett. **77**, 4250 (2000).
[8] C. H. Chia, T. Makino, K. Tamura, Y. Segawa, M. Kawasaki, A. Ohtomo, and H. Koinuma, Appl. Phys. Lett. **82**, 1848 (2003).
[9] J. A. Davis, L. V. Dao, X. Wen, P. Hannaford, V. A. Coleman, H. H. Tan, C. Jagadish, K. Koike, S. Sasa, M. Inoue, and M. Yano, Appl. Phys. Lett. **89**, 182109 (2006).
[10] Y. Harada, H. Kondo, and S. Hashimoto, J. Appl. Phys. **98**, 093510 (2005).
[11] X. Chen, K. Ruan, G. Wu, and D. Bao, Appl. Phys. Lett. **93**, 112112 (2008).
[12] D. Gupta, M. Anand, S. W. Ryu, Y. K. Choi, and S. Yoo, Appl. Phys. Lett. **93**, 224106 (2008).
[13] D. C. Reynolds, D. C. Look, B. Jogai, C. W. Litton, G. Cantwell, and W. C. Harsch, Phys. Rev. B **60**, 2340 (1999).
[14] B. Gil, Phys. Rev. B **64**, 201310 (2001).
[15] B. Gil, A. Lusson, V. Sallet, S.-A. S. Hassami, R. Triboulet, and P. Bigenwald, Jpn. J. Appl., Phys. Part 2 **40**, L1089 (2001).
[16] Ü. Özgür, Y. I. Alivov, C. Liu, A. Teke, M. A. Reshchikov, S. Doğan, A. Avrutin, S.-J. Cho, and H. Morkoc, J. Appl. Phys. **98**, 041301 (2005).
[17] S. Adachi, K. Hazu, T. Sota, S. Chichibu, G. Cantwell, D. C. Reynolds, and C. W. Litton, Phys. Status Solidi C **2**, 890 (2005).
[18] C. Klingshirn, Phys. Status Solidi B **71**, 547 (1975).
[19] A. Yamamoto, K. Miyajima, T. Goto, H. J. Ko, and T. Yao, J. Appl. Phys. **90**, 4973 (2001).
[20] P. Zu, Z. K. Tang, G. K. L. Wong, M. Kawasaki, A. Ohtomo, H. Koinuma, and Y. Segawa, Solid State Commun. **103**, 459 (1997).
[21] Y. Kayanuma, Phys. Rev. B **38**, 9797 (1988).